Development of High-Efficiency Permanent Magnet Synchronous Generator for Motorcycle Application

Toshihiko Noguchi, Yuki Kurebayashi, Tetsuya Osakabe †, and Toshihisa Takagi †
Shizuoka University and Suzuki Motor Corporation †
noguchi.toshihiko@shizuoka.ac.jp, kurebayashi.yuki.16@shizuoka.ac.jp

***Abstract*-High-efficiency design of a permanent magnet synchronous generator is discussed in this paper. The application of the generator is a motorcycle, and improvement of the efficiency is focused on to reduce the fuel consumption of the motorcycle. The generator has an outer rotor configuration, and has a single-phase winding for compact motorcycles and three-phase windings for large motorcycles on the stator. There are a lot of restrictions on designing this kind of auxiliary machines because of the cost, mechanical and electrical compatibility with conventional motorcycles, productivity, and so forth. The new design is conducted through the FEM based three-dimensional electromagnetic analysis, and approximately 10-% power loss is reduced through the development, which can contribute the mileage improvement or the reduction of the fuel consumption of the motorcycle.**

INTRODUCTION

Engine efficiency of motorcycles has been improved so far by directly increasing the combustion efficiency. One of the epoch-making improvements was a drastic change of the engine operation from two-stroke cycle to four-stroke cycle in the past. Another improvement has been achieved with a high-performance catalyzer and a fuel injection system, which contribute not only the combustion efficiency improvement but also quality improvement of the exhaust gas. Many efforts are still being made for further improvement of the mileage or the fuel consumption [1]. In recent years, great advancement of the mileage improvement is expected from the view point of further environmental conservation because of the rapid motorcycle market growth in Asia. As described above, it goes without saying that the combustion efficiency improvement and the mechanical power loss reduction are indispensable to achieve low fuel consumption of the motorcycles. These improvements, however, are somehow approaching to a technical limit, and it is rather difficult to overcome the limit. Therefore, auxiliary machines have been focused on to improve the total efficiency of the motorcycle and to reduce the fuel consumption [2]. The typical auxiliary electric machine is a permanent magnet (PM) synchronous generator to charge a 12-V battery and to feed electric equipment such as lamps and meters.

On the other hand, a commonly used rectifier to charge the 12-V battery is a short circuit type, which makes the generator windings short when the battery is fully charged; thus, the generator has been designed to have a high synchronous inductance to reduce the power losses when the windings are shorted. However, an open type rectifier is recently used for the motorcycle, which opens the generator windings when the battery state of charge (SOC) is high enough. Assuming use of the open type rectifier, the paper discusses development of the new generator that can improve overall fuel efficiency of the motorcycle [3] [4].

CONVENTIONAL MOTORCYCLE GENERATOR

A. Overview of Conventional Generator

Fig. 1 and TABLE I show photographs and specifications of a conventional generator for a motorcycle. As can be seen in the figure, the generator is a PM synchronous generator with a 12-pole outer rotor and an 18-slot stator with three-

TABLE I. SPECIFICATIONS OF CONVENTIONAL GENERATOR.

Normalized rotor diameter	1
Normalized stator diameter	0.824
Normalized axial length of stator core	0.144
Normalized air gap length	5.73×10^{-3}
Coil diameter	1.15 mm
Number of coil-turns per pole	42
Winding resistance for one phase	0.30 Ω
Normalized thickness of iron core plate	3.82×10^{-3} (EMSP)
Normalized thickness of iron core plate	9.16×10^{-3} (SPCC)

Fig. 1. Photographs of conventional generator for motorcycle.

978-1-5090-2364-6/17/$31.00 ©2017 IEEE

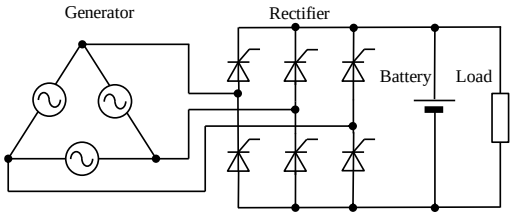

Fig. 2. Electric circuit diagram of auxiliary equipment of motorcycle.

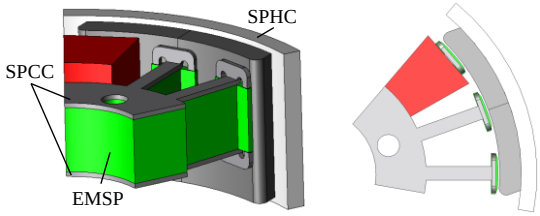

Fig. 3. Simulation model of conventional generator.

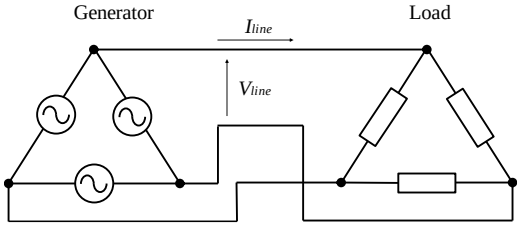

Fig. 4. Circuit diagram for measuring generator operation characteristics.

phase concentrated windings [5]. The rotor is directly connected to a crankshaft of the engine, and rotates synchronously with the engine. The unique point of the machine is a stator iron core structure, which uses SPCC plates sandwiching the laminated electromagnetic steel plates (EMSP) and the SPCC plates are folded by 90 deg toward the axial direction at the teeth edge. This construction seems to be effective to retrieve more magnetic flux from the PM on the rotor.

An electric circuit diagram for the motorcycle auxiliary system is shown in Fig. 2, including the generator and a thyristor full-bridge rectifier. The rectifier is used in two operating modes, i.e., an open mode and a conduction mode. All the thyristors are turned off in the open mode, and are turned on in the conduction mode. These modes are altered to regulate the battery voltage around 13 V on the basis of the duty cycle control. The aim of the machine design is to reduce the power losses of the generator with the thyristor rectifier at a designated operating point. Therefore, some experimental tests in the following sections have been conducted under the condition of the 13-V DC-bus voltage regulated by an electronically controlled load so as not to turn off the thyristor rectifier.

Figs. 3 and 4 represent the 3-D model of the conventional generator and the circuit diagram used for evaluation of only the generator, respectively. In the case of operation characteristic measurement of only the generator, three-phase variable resistive loads are simply connected to the generator.

B. Operation Characteristics of Conventional Generator

Figs. 5 (a) to (e) show various operation characteristics of the conventional generator at 3000 r/min, comparing the

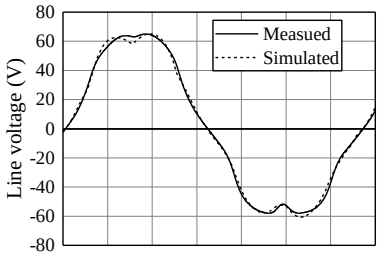

(a) No-load line-to-line voltage waveform at 3000 r/min.

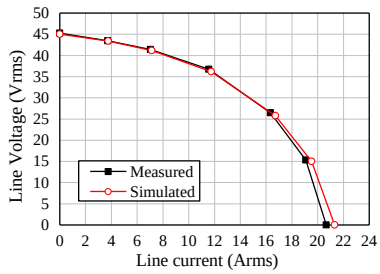

(b) V-I characteristics.

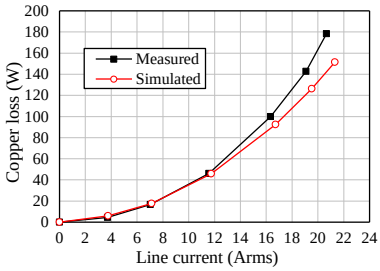

(c) Copper loss characteristics.

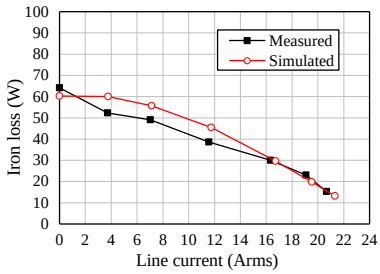

(d) Iron loss characteristics.

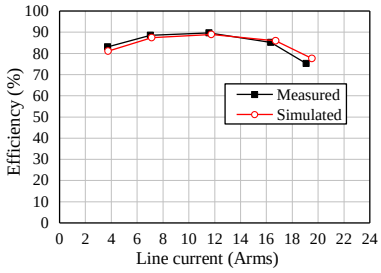

(e) Efficiency characteristics.

Fig. 5. Operation characteristics of conventional generator.

experimental test results with FEM based electromagnetic analysis results. A simulator JSOL's JMAG-Designer 16 ® is used for the FEM based electromagnetic analysis [6]. The rotating speed of 3000 r/min has been specified because this operating point is the most frequent condition in the motorcycle driving modes. Temperature of the PM and the

winding resistance has been kept constant at every measurement point through the computer simulations. It can be found from the figures that there are some errors between the analysis and the experimental results in a heavy load range. The errors seem to be caused by the winding resistance variation due to its temperature rise in the experiments. As can be seen in the Fig. 5 (c), the dominant power loss is copper loss when the rectifier is in the conduction mode. The iron loss, however, is reduced as shown in Fig. 5 (d) because of the armature reaction magnetic flux that cancels the PM flux, which results in the magnetic flux density reduction in the stator iron core.

Fig. 6 (a) shows power losses in the two operation modes of the rectifier at 3000 r/min. The copper loss is dominant in the conduction mode of the rectifier whereas only the iron loss is measured in the open mode. The detailed analysis result of the iron losses in the open mode at 3000 r/min is indicated in Fig. 6 (b), and the iron loss analysis results with respect to the rotation speeds are depicted in Fig. 6 (c). As shown in Fig. 6 (b), the most part of the iron losses appears in the stator iron core, especially as eddy current losses. It should be noted that the eddy current loss of the SPCC plates is significant for their small physical volume among all iron losses. Fig. 7 shows a 3-D FEM analysis result of the SPCC plate at 3000 r/min, where the eddy current loss distribution is indicated. Since the thickness of each SPCC plate is 2.4 times of the laminated EMSP and the SPCC plate is folded in the axial direction at the end of the tooth as described previously, the eddy current loss concentrates on the SPCC plate. Fig. 8 shows output current characteristics of the rectifier under the condition of a 13-V constant battery voltage and a saturated machine temperature. The simulation and the measured results agree very well, and the output current is limited under 28 A even in the higher speed range because of increase of the synchronous reactance.

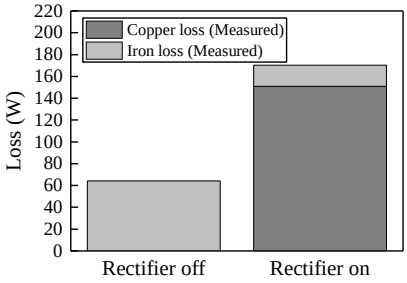

(a) Power losses at 3000 r/min.

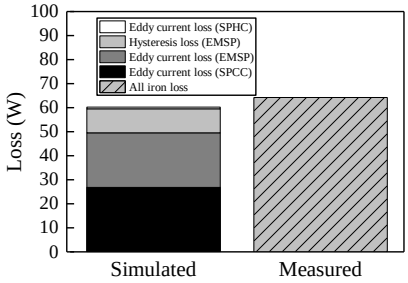

(b) Details of no-load iron losses at 3000 r/min.

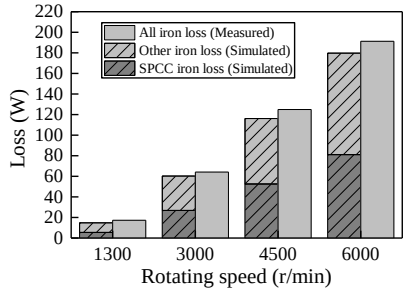

(c) Power loss characteristics with respect to rotating speed.

Fig. 6. Detailed iron loss characteristics of conventional generator.

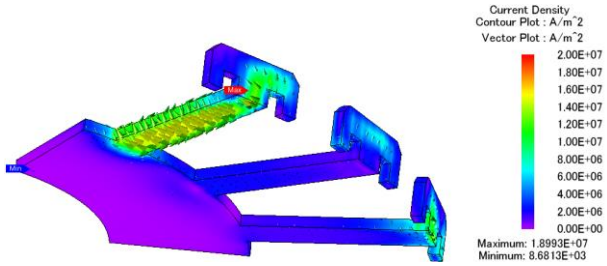

Fig. 7. Eddy current loss generated in SPCC plate at 3000 r/min.

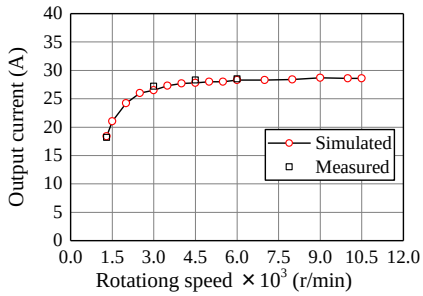

Fig. 8. Rectifier output current characteristics of conventional generator.

IMPROVED DESIGN OF MOTORCYCLE GENERATOR

The rotor back yoke has not been modified in the new design because the mechanical compatibility with the conventional model is important. In addition, some different materials for the PM are available, but it is difficult to change the PM size due to the compatibility reason. The improved generator has newly been designed according to the following restrictions [7]:

1) less than 400-V output voltage at 10500 r/min;
2) 18.5-A or more battery input current at 1300 r/min; and
3) less than 35-A battery input current at 10500 r/min.

The above design restrictions are imposed due to the thyristor rectifier absolute ratings and the power requirement of the actual motorcycle. In the first step of the new design process, the SPCC plates are eliminated from the stator iron core, and higher quality EMSP is employed instead of the SPCC to reduce the iron loss by 40 %. Since the copper loss takes major part of the total power loss during the conduction mode of the thyristor rectifier, the diameter of the stator windings are designed larger to reduce the copper loss. In order to make the thicker windings possible, the slot cross section is enlarged by 7.1 % by making the slot deeper than the

conventional model. It is necessary to increase the axial length of the stator iron core to compensate for the reduced magnetic flux due to the elimination of the SPCC plates. The newly designed stator axial length is 5.8 % longer than that of the conventional model, resulting in the same weight of the stator iron core owing to the enlarged slot areas. As for the PM, the class-5 or the class-6 ferrite PM has been employed to mount on the outer rotor with a stainless steel (SUS) sleeve. The SUS sleeve is attached on the PM surface for its mechanical reinforcement whereas it has a drawback to generate additional eddy current loss.

TABLE II shows a relationship between the axial length of the PM and the electromotive force at 3000 r/min, where all of the PM length are longer than the stator axial length. As indicated in the table, the electromotive force strongly depends on the PM overhang, but saturates even though the PM axial length becomes longer than 32 mm. Therefore, the 32-mm long PM in the axial length has been selected.

The number of the poles has been determined by comparing the total power losses between the 12-pole and the 20-pole machines with the same 18-slot stator. Fig. 9 is estimated stator iron losses in no load condition of the 18-pole and the 20-pole machines at several rotating speeds. It can be seen that the 12-pole machine is superior to the 20-pole one from the viewpoint of the stator iron loss reduction.

The peak-to-peak output voltage $V_{p\text{-}p}$ at the 10500-r/min maximum rotating speed has to be limited to 400 V because of the maximum voltage rating of the thyristor rectifier. On the other hand, the output current at the 1300-r/min lowest speed has to be over 18.5 A to charge the battery even in the idling situation. Therefore, it is necessary to reduce the synchronous inductance to satisfy the above requirements. One of the effective methods of reducing the inductance is adjustment of the slot opening, which has an impact on the leakage magnetic flux. In other words, the number of the flux linkage to the stator windings is affected by the slot opening, so the number of the winding turns must be adjusted to satisfy the first requirement. Fig. 10 (a) shows the relationship between the slot opening width and the number of the winding turns, which makes $V_{p\text{-}p}$ at no load less than 400V. In addition, Fig. 10 (b) indicates $V_{p\text{-}p}$ at 10500 r/min under the conditions shown in Fig. 10 (a), i.e., combinations of the number of the winding turns and the slot opening width. Figs 11 (a) and (b) are output current characteristics with respect to the slot opening width at 1300 r/min and 10500 r/min. Fig. 11 (a) shows a relationship between the number of the winding turns per slot and the slot opening width, and Fig. 11 (b) shows a characteristic of the terminal voltage $V_{p\text{-}p}$ at 10500 r/min with respect to the number of the turns. The number of the turns can be determined at every slot opening width from the figure, so it has been checked whether the second and the third design requirements are satisfied or not. The output current characteristic with respect to the slot opening width is shown in Fig. 11. It is confirmed from the figure that the synchronous inductance increases and the leakage inductance deceases as the number of the winding turns increases and that the current monotonically goes up with the slot opening width. The appropriate slot opening widths that satisfy the design requirements are 6 mm for 36 T, 7 mm for 37 T, 8 mm for 38 T, and 9 mm for 39 T. Fig. 12 shows comparison of the total iron losses and their contents for every slot opening width from 4 to 9 mm. As can be found in the figure, 7-mm slot opening width is the best choice to reduce the total iron loss. Since the generator must have a marginal output characteristic, a model with 7-mm slot opening width and 37-turn windings is employed. The

TABLE II. EFFECT OF PM OVERHANG.

Axial length of PM	No-load voltage at 3000 r/min
37 mm	40.98 V (0 %)
32 mm	40.18 V (-2.0 %)
25 mm	37.29 V (-9.0 %)

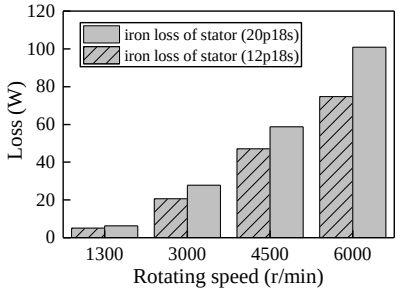

Fig. 9. Comparison of no-load iron losses.

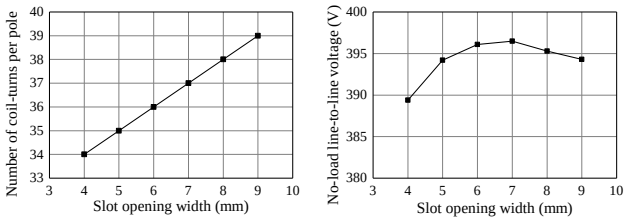

(a) Number of turns to limit voltage. (b) Voltage at 10500 r/min.

Fig. 10. Number of winding turns to limit no-load output voltage less than 400 V at 10500 r/min.

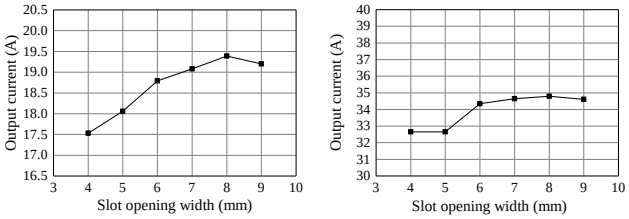

(a) 1300 r/min. (b) 10500 r/min.

Fig. 11. Output current characteristics with respect to slot opening width.

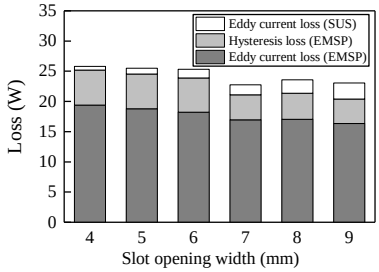

Fig. 12. Iron loss characteristics with respect to slot opening width.

TABLE III. SPECIFICATIONS OF IMPROVED DESIGN GENERATOR.

Normalized rotor diameter	1
Normalized stator diameter	0.824
Normalized axial length of stator core	0.153
Normalized air gap length	7.63×10^{-3}
Coil diameter	1.20 mm
Number of coil-turns per pole	37
Winding resistance for one phase	0.22 Ω
Normalized thickness of iron core plate	3.82×10^{-3} (EMSP)

Fig. 13. Photographs of improved design generator for motorcycle.

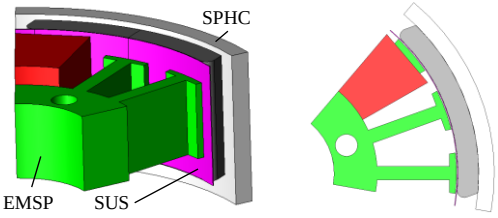

Fig. 14. Simulation model of improved design generator.

diameter of the coils has been increased by 0.05 mm owing to the slot area expansion and the reduction of the number of the turns, resulting in lowering the winding resistance per phase from 0.30 to 0.22 Ω. TABLE III shows the final major specifications of the newly designed generator. An SUS sleeve is attached to the PM for mechanical reinforcement and for preventing the PM from chipping in an assembly process. An air gap is slightly wider than that of the conventional model due to the sleeve although the rotor inner diameter has not been changed from the conventional one.

PROTOTYPE GENERATOR AND TEST RESULTS

Figs. 13 and 14 are photographs of the newly designed prototype and its 3-D model for electromagnetic analysis, respectively. Figs. 15 (a) to (e) show operation characteristics of the prototype generator at 3000 r/min, comparing the experimental results with the analysis results. As can be seen in the figures, the five characteristics are as what are designed, and both of the copper loss and the iron loss are remarkably reduced, which improves significantly the efficiency of the generator.

Fig. 16 shows no-load iron loss analysis results at 3000 r/min. The extra iron loss is generated in the SUS sleeve,

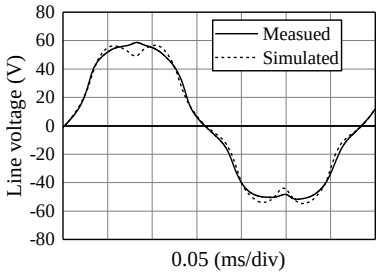

(a) No-load line-to-line voltage waveform at 3000 r/min.

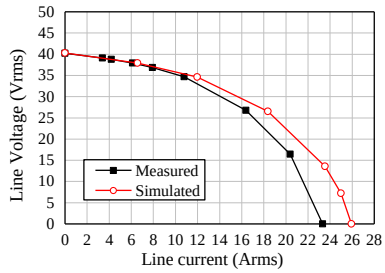

(b) V-I characteristics.

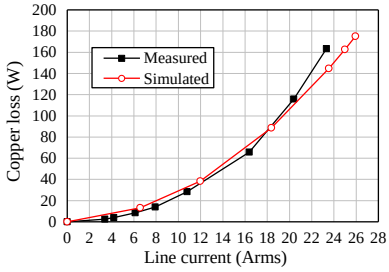

(c) Copper loss characteristics.

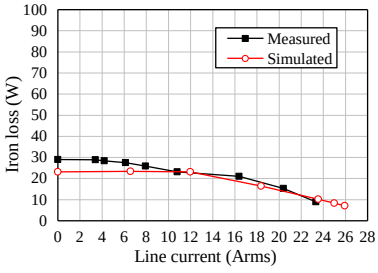

(d) Iron loss characteristics.

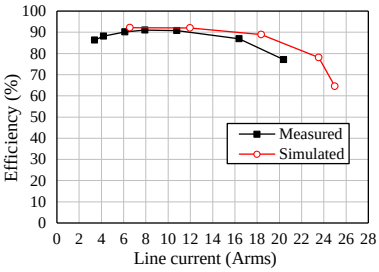

(e) Efficiency characteristics.

Fig. 15. Operation characteristics of improved deign generator.

which is also confirmed in the 3-D electromagnetic analysis result shown in Fig. 17. The figure shows an eddy current loss distribution on the sleeve, and it can be seen that the eddy current loss is mainly generated between the stator teeth. Fig. 18 is comparison of the loss analysis results in the open and the conduction modes of the rectifier between the

conventional generator and the prototype. The total power loss of the prototype is remarkably reduced regardless of the rectifier modes. Fig. 19 is V-I characteristics of the conventional generator and the prototype at the idling speed, where it is found that the short-circuit line current is increased owing to the low synchronous inductance design of the prototype. Fig. 20 shows output current characteristics when the battery voltage is kept at 13 V. It is confirmed from the figure that the output currents of the prototype are less than the predicted values obtained by the electromagnetic analysis, and that the characteristic does not satisfy the design requirements. The reason why the output current of the prototype has been less than the target values is temperature rise of the PM and voltage drops in the wire harness connecting the rectifier to the battery. Therefore, it is desired to redesign the improved generator eligible to the target output characteristics, taking the above issues into account.

CONCLUSION

This paper has discussed a high-efficiency design of a motorcycle generator. As a result of the investigation described above, it is possible for the prototype to reduce the total loss by 54.8 % (35.2 W) under no load (the open mode of the rectifier) condition and by 10.1 % (17.3 W) under loaded (the conduction mode of the rectifier) condition at the rotation speed of 3000 r/min, compared with the conventional generator. Although the prototype surpasses the conventional model from angles of the power losses and the efficiency, the required specifications are not satisfied slightly yet; hence, the further investigation will be made for a future work.

REFERENCES

[1] A. Triwiyatno, E. W. Sinuraya, J. D. Setiawan, and S. Munahar, "Smart Controller Design of Air to Fuel Ratio (AFR) and Brake Control System on Gasoline Engine," *2nd International Conference on Information Technology, Computer, and Electrical Engineering*, 2015.

[2] M. Comanescu, A. Keyhani, and M. Dai, "Design and Analysis of 42-V Permanent-Magnet Generator for Automotive Applications," *IEEE Transactions on Energy Conversion*, vol. 18, no. 1, 2003, pp. 107-112.

[3] T. Osakabe, and T. Takagi "Study on Efficiency Improvement of Compact Generator for Motorcycle," *SAE Conference Technical Paper*, 2014-32-0138, 2014.

[4] D. Takeuchi, T. Noguchi, T. Osakabe, S. Sako, and T. Takagi, "Study on Efficiency Improvement of Compact Generator for Motorcycle," *IEEJ Industry Applications Conference*, vol. III, 2013, pp. 211-212.

[5] A. Olano, V. Moreno, J. Molina, and I. Zubia, "Design and Construction of an Outer-Rotor PM Synchronous Generator for Small Wind Turbines; Comparing Real Results with Those of FE Model," *18th International Conference on Electrical Machines*, 2008.

[6] M. Jenal, E. Sulaiman, M. Z. Ahmad, S. N. U. Zakaria, W. M. Utomo, S. A. Zulkifli, and A. A. Bakar, "Design Study of Single and Three-Phase Synchronous Generator Using J-MAG Designer," *International Conference on Clean Energy and Technology*, 2013.

[7] P. Eklund and S. Eriksson, "Air Gap Magnetic Flux Density Variations Due to Manufacturing Tolerances in a Permanent Magnet Synchronous Generator," *22nd International Conference on Electrical Machines*, 2016.

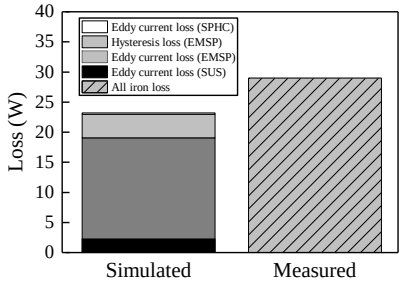

Fig. 16. Details of no-load iron losses at 3000 r/min.

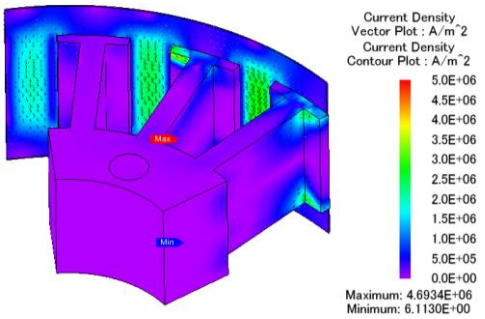

Fig. 17. Eddy current distribution generated in stainless steel sleeve.

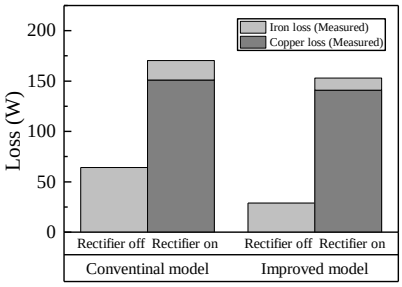

Fig. 18. Power loss comparison between conventional and improved models in two operation modes of rectifier.

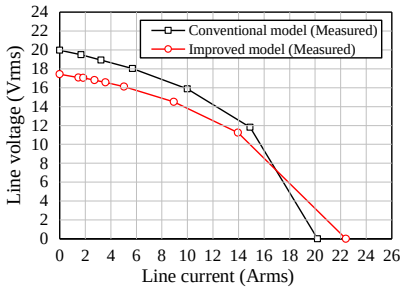

Fig. 19. V-I characteristics of conventional and improved models at 1300 r/min (idling speed).

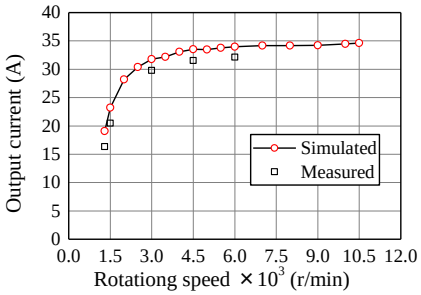

Fig. 20 Rectifier output current characteristics of improved generator.